Influence of the Nuclear Electric Quadrupolar Interaction on the Coherence Time of Hole and Electron Spins Confined in Semiconductor Quantum Dots

J. Hackmann,[1] Ph. Glasenapp,[2] A. Greilich,[2] M. Bayer,[2] and F. B. Anders[1]
[1]*Theoretische Physik 2, Technische Universität Dortmund, D-44221 Dortmund, Germany*
[2]*Experimentelle Physik 2, Technische Universität Dortmund, D-44221 Dortmund, Germany*
(Received 27 April 2015; published 9 November 2015)

The real-time spin dynamics and the spin noise spectra are calculated for p and n-charged quantum dots within an anisotropic central spin model extended by additional nuclear electric quadrupolar interactions and augmented by experimental data. Using realistic estimates for the distribution of coupling constants including an anisotropy parameter, we show that the characteristic long time scale is of the same order for electron and hole spins strongly determined by the quadrupolar interactions even though the analytical form of the spin decay differs significantly consistent with our measurements. The low frequency part of the electron spin noise spectrum is approximately $1/3$ smaller than those for hole spins as a consequence of the spectral sum rule and the different spectral shapes. This is confirmed by our experimental spectra measured on both types of quantum dot ensembles in the low power limit of the probe laser.

DOI: 10.1103/PhysRevLett.115.207401 PACS numbers: 78.67.Hc, 72.25.-b, 78.20.Ls, 78.55.-m

Introduction.—The promising perspective of combining traditional electronics with novel spintronics devices leads to intensive studies of the spin dynamics of a single electron (n) or hole (p) confined in a semiconductor quantum dot (QD) [1–4]. In contrast to defects in diamonds [5,6], such QDs may be integrated into conventional semiconductor devices. While the strong confinement of the electronic wave function in QDs reduces the interaction with the environment and suppresses electronic decoherence mechanisms, it simultaneously enhances the hyperfine interaction between the confined electronic spin and the nuclear spins formed by the underlying lattice.

Generally it is believed [3,4,7,8] that the hyperfine interaction dominates the spin relaxation in QDs. The s-wave character of the electron-wave function at the nuclei leads to an isotropic central spin model (CSM) [9] for describing the electron-nuclear hyperfine coupling, while for p-charged QDs, the couplings to the nuclear spins can be mapped onto an anisotropic CSM [4,10]. Since the coupling constants for p-charged QDs are reduced compared to the n-charged QDs [4,10], and additionally a large anisotropy factor $\Lambda > 1$ suppresses the spin decay of the S_z component [4,10], p-charged QDs have been considered as prime candidates for long lived spin excitations in spintronics applications.

Experimentally, however, there is evidence for comparable spin-decay times of the S_z components [11–15] in p- and n-charged QDs; hence, the anisotropic CSM provides only an incomplete description of the relevant spin-relaxation processes in such systems.

In this Letter, we resolve this puzzle by investigating the effect of an additional realistic nuclear electric quadrupolar interaction term (QC) [16] onto the spin decoherence. All stable Ga and As isotopes have a nuclear spin $I = 3/2$ which is subject to a quadrupolar splitting in electric field gradients that occur in self-assembled QDs by construction and couples to the quadrupole moment of the nuclei [16,17]. Previously simplified assumptions have been made [18–20], or the problem has been mapped on an effective $I = 1/2$ model in a random magnetic field [21] which cannot capture the full dynamics since it violates Kramers degeneracy in zero field. Therefore, we have taken into account the proper In dependent anisotropy and realistic strain field orientations estimated by a recent microscopic calculation [22]. Although the short-time dynamics of p- and n-charged QDs are significantly different [4,23], we show that the long time dynamics is governed by the same time scale set by the quadrupolar interactions in agreement with our experimental data presented below.

Over the last decade, an intuitive picture for the central spin dynamics interacting isotropically with a spin bath via hyperfine interaction has emerged. The separation of time scales [7]—a fast electronic precession around an effective nuclear magnetic field, and slow nuclear spin precessions around the fluctuating electronic spin—has motivated various semiclassical approximations [1,7,21,24–26] which describe the short-time dynamics of the central spin polarization well. As can be shown rigorously [27] the CSM predicts a finite nondecaying spin polarization [7,28,29] whose lower bound depends on the distribution function of the hyperfine couplings and is only linked to conservation laws. In semiclassical theories [7,28] it is given by a third of the initial spin polarization leading to a large spectral weight at zero frequency in the spin-noise spectrum. The absence of such a zero-frequency contribution in experiments [11,30–32] provides strong evidence that the CSM is incomplete and additional interactions such as QC play an important role in the decoherence mechanism.

In this Letter, we have employed a fully quantum mechanical approach, based on a Chebyshev polynomial technique (CET) [33–35], to an extended anisotropic spin model. In order to include QC, we simulate $I = 3/2$ nuclear spins. Within the CET method the largest accessible time scale or lowest frequency is linearly connected to the Chebyshev polynomial order. All technical details can be found in Refs. [23,35].

Modeling a quantum dot.—In the absence of an external magnetic field, the dynamics of a single p- and n-charged QD is described by the Hamiltonian $H = H_{\mathrm{CSM}} + H_{\mathrm{QC}}$. The coupling of the central electron or hole spin $\vec{S}$ to the nuclear spin bath can be casted [10,36] into the anisotropic CSM Hamiltonian H_{CSM}

$$H_{\mathrm{CSM}} = \sum_{k=1}^{N} A_k \left(S^z I_k^z + \frac{1}{\lambda} (S^x I_k^x + S^y I_k^y) \right). \quad (1)$$

$\vec{I}_k$ denotes the nuclear spin of the kth nucleus, and N is the number of nuclear spins. The anisotropy parameter λ of the spin-flip term [10] distinguishes between electron ($\lambda = 1$) and hole spins, where $1 < \lambda < \infty$ applies depending on the mixture between light and heavy holes. Because of the enlarged Hilbert space of 2^{2N+1} for $I = 3/2$, we have restricted ourselves to $N = 10$ in the numerics. This, however, reproduces the previous results [23] for $N = 20$ nuclear spins with $I = 1/2$ in the absence of the QC term. While for $\lambda = 1$ the total angular momentum $\vec{J}_{\mathrm{tot}} = \vec{S} + \sum_k \vec{I}_k$ and, therefore, J_{tot}^2 is conserved, only J_{tot}^z remains as good quantum number for $\lambda \neq 0$.

The energy scale $A_s = \sum_k A_k$ is expected to be of $O(10)$ μeV for electrons and approximately one order of magnitude smaller for holes [10]. The coupling constants A_k are proportional to the squared absolute value of the electron or hole envelope-wave function at the kth nucleus—for details concerning a realistic modeling of the considered set of A_k entering our numerics, see Ref. [23].

The additional quadrupolar term [16] in H

$$H_{\mathrm{QC}} = \sum_{k=1}^{N} q_k \left[(\vec{I}_k \vec{n}_k^z)^2 - \frac{I(I+1)}{3} \right] + \frac{q_k \eta}{3} [(\vec{I}_k \vec{n}_k^x)^2 - (\vec{I}_k \vec{n}_k^y)^2] \quad (2)$$

originates from electric field gradients in self-assembled QDs that couple to the nuclear electric quadrupole moment and are of crucial importance for the long-time dynamics of the central spin. The coupling constant q_k is mainly governed by the second order derivative of the strain induced electric potential V [16]. The local z direction at the kth nucleus is denoted by the normalized orientation vector $\vec{n}_k^z$ which refers to the eigenvector corresponding to the largest eigenvalue of the quadrupolar electric interaction tensor. The unit vectors $\vec{n}_k^{x/y}$ complete the local orthonormal basis. Since J_{tot}^z does not commute with H_{QC} in general, the lack of total spin conservation also favors the decoherence of the central spin.

The asymmetry parameter $\eta = (V_{xx} - V_{yy})/V_{zz}$ is commonly neglected in the literature [18,19,21,52]. Recent concentration dependent microscopic calculations of the nuclear electric quadrupolar couplings [22] in self-assembled $\mathrm{In}_x\mathrm{Ga}_{1-x}\mathrm{As}$ QDs as well as experimental measurements [53], however, have found values up to $\eta \approx 0.5$ depending on the In concentration in the QD. Therefore, we have included a finite $\eta = 0.5$ in our calculations.

The individual coupling constants q_k are expected to be up to $O(1)$ neV [22], but only those q_k are relevant for the central spin dynamics where simultaneously A_k is of the same order of magnitude or larger. We define $A_q = \sum_k q_k$ as a measure of relevant total quadrupolar coupling strength which is expected to be in the range of 1–100 μeV restricting the largest q_k to $q_{\max}$. The ratio $Q_r = A_q/A_s$ determines the relative strength of the QC.

For our simulations, we generate random orientation vectors $\vec{n}_k^z$ for each nucleus in our calculation whose deviation angles are restricted to $\theta_z \leq 35°$ in accordance to the average deviation angle $\bar{\theta}_z \approx 25°$ between the growth direction of the dot and the orientation vectors $\vec{n}_k^z$ for $\mathrm{In}_{0.4}\mathrm{Ga}_{0.6}\mathrm{As}$ found by Bulutay [22]. The coupling constants q_k have been generated randomly from a uniform distribution $q_k/q_{\max} \in [0.5:1]$.

For $\eta = 0$, H_{QC} partially lifts fourfold degenerate nuclear spin states. Pinning $\vec{n}_k^z$ to the growth direction, decoherence of the central spin would be suppressed with increasing q_k. A distribution of $\vec{n}_k^z$ due to the inhomogeneous strain fields [22] favors the decoherence. Including a finite η further enhances the decoherence due to the $\eta[(I_k^+)^2 + (I_k^-)^2]$ term in H_{QC}.

The fluctuations of the transversal and longitudinal component of the unpolarized nuclear spin bath, referred to as Overhauser field, define the time scale $T^* = \lambda/\sqrt{[4I(I+1)/3]\sum_{k=1}^N A_k^2}$ governing the short-time evolution of the central spin [7,23] in the absence of H_{QC}. We have used this natural time scale to define the dimensionless Hamiltonian $\tilde{H} = T^* H$. Two factors in the definition of T^* suggest a longer lifetime for hole spin coherence than for electron spins: (i) the coupling constants A_k for holes are typically one order of magnitude smaller [10] than for electrons, and (ii) increasing the parameter $\lambda \geq 1$ to larger values suppresses flips of the central spin. Both factors enter the time scale linearly, yielding an expected lifetime increase of a factor $\sim 10\lambda$ for holes compared to electrons. However, when the spin-flip term in H_{CSM} becomes of the order of H_{QC}, this argument fails and the long time decay rate will be strongly influenced by the QC for p-doped QDs as we will demonstrate below.

Definition of the spin-noise function.—The Fourier transformation $S(\omega)$ of the fluctuation function $S(t) = \frac{1}{2}[\langle S^z(t) S^z \rangle + \langle S^z S^z(t) \rangle] - \langle S^z \rangle^2$ corresponds to the experimentally measured [11,30–32] spectral power density (see below for experimental details). For very small probe laser intensity, all expectation values can be calculated using the equilibrium density operator. Hence, $S(t)$ is symmetric in time, and $S(\omega)$ is given by

$$S(\omega) = \int_{-\infty}^{\infty} S(t)e^{-i\omega t}dt = \int_{-\infty}^{\infty} S(t)\cos(\omega t)dt. \quad (3)$$

From these definitions, we obtain the sum rule

$$\int_{-\infty}^{\infty} \frac{d\omega}{2\pi} S(\omega) = S(0) = \langle (S^z)^2 \rangle - \langle S^z \rangle^2 \quad (4)$$

for the spin-noise spectrum. In the absence of an external magnetic field, its value is fixed to $1/4$ for a QD filled with a single spin.

Since all experiments are performed in the high-temperature limit, the inverse temperature $\beta = 0$, and a constant density operator has been used in all numerical calculations. Then the spin autocorrelation function $S(t)$ also describes the spin decay of an initially fully polarized central spin [23] interacting with an unpolarized nuclear spin bath, i.e., $S(t) = \langle S_z(t) \rangle /2$.

Results.—The two-stage dynamics of $S(t)$ for electron spins is clearly visible in Fig. 1(a). The initial short-time decay on the scale T^* to a plateau of approximately $S(0)/3$ is only governed by the Overhauser field [7] and not influenced by QC. Here, we have used the time scale of $T^* = 1$ ns [15]. The second stage of the spin decay is well separated from the first for small values of Q_r and is governed by QC. The shape of our curves agrees

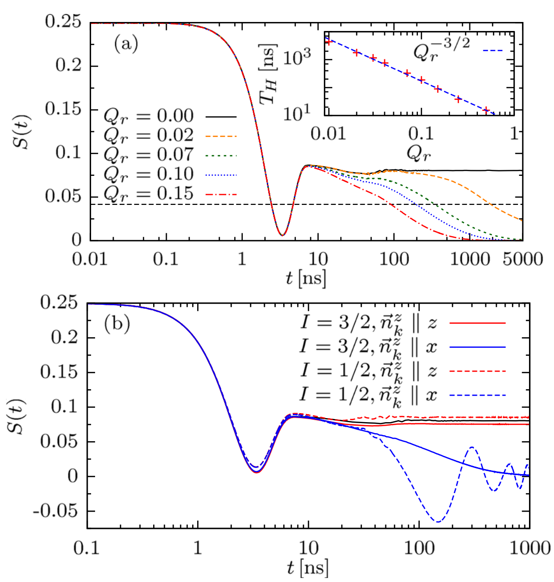

FIG. 1 (color online). (a) $S(t)$ of a single electron confined in an InGaAs semiconductor QD for various values of the parameter $Q_r = A_q/A_s$. Inset: dependence of the lifetime T_H defined by the crossing of the black dashed line and $S(t)$ at large times $t \sim O(10^2\text{–}10^3)$ ns, on the ratio Q_r, which can be approximated by a power law $\propto Q_r^{-3/2}$. (b) Spin decay for fixed $\vec{n}_k^z$ orientation, $\eta = 0$ and $Q_r = 0.1$ for the full H_{QC} and the mapping onto an effective $I = 1/2$ model [21]. The $Q_r = 0$ line (black) of (a) has been added as reference.

remarkably with the data of Bechtold *et al.* [15]: $Q_r \approx 0.06\text{–}0.1$ seems to be an adequate choice for electrons confined in those $In_{0.5}Ga_{0.5}As$ QDs.

We have defined a second time scale T_H at which $S(t)$ has dropped to the value $S(0)/6$ indicated by the black dashed line in Fig. 1(a) (half the plateau) and have plotted the dependency of the lifetime T_H on Q_r in the inset. $T_H(Q_r)$ approximately obeys a power law $\propto Q_r^{-3/2}$.

To (i) reveal the difference between the correct QC term and the effective $I = 1/2$ model [21] and (ii) demonstrate the angular dependence of $S(\omega)$ on the orientation of $\vec{n}_k^z$, we set $\eta = 0$ in Fig. 1(b) and focus on uniform $\vec{n}_k^z$. Starting with $\vec{n}_k^z = \vec{e}_z$ and expanding $S(t)$ in powers of H generates a linear and a quadratic term in QC with opposite signs in leading order. Consequently, a nonmonotonic dependency of the spin decay on QC is found: for small Q_r the decoherence is enhanced, while for large Q_r decoherence is suppressed. In the effective $I = 1/2$ model [21], however, the linear term is absent, and the coherence is always enhanced for all Q_r as demonstrated in the full numerical calculation shown in Fig. 1(b) by comparison to the $Q_r = 0$ case. Furthermore, while the $I = 1/2$ model underestimates the spin decay in the z direction, it predicts unphysical oscillations for $\vec{n}_k^z = \vec{e}_x$. Switching on the quadrupolar asymmetry η in the full model increases the dephasing and has a similar effect as increasing the angle between $\vec{e}_z$ and $\vec{n}_k^z$.

Figure 2(a) shows the spin-noise spectra $S(\omega)$ for n-doped QDs for various Q_r. The peak at around 100 MHz originates from the fluctuation of the Overhauser field and is only slightly influenced by the variation of Q_r. The QC dominates the low frequency spectrum: an increase of Q_r broadens the peak width and induces a change of decay at intermediate frequencies in $S(\omega)$.

Now we focus on p-charged QDs. Since the overall QC strength A_q does not depend on the charge of the QD while A_s is decreasing by one order of magnitude when turning from electrons to holes, the ratio Q_r is increasing by one order of magnitude at fixed A_q. An increase of Q_r yields a decrease of T_H/T^* when turning from electrons to holes. At the same time T^* is increasing by a factor 10λ so that T_H will be of the same order of magnitude for electrons and holes.

Figure 2(b) shows $S(\omega)$ for p-charged $In_{0.4}Ga_{0.6}As$ QDs for three sets of parameters λ and Q_r. Here we assumed a reduction of A_s by a factor of 10 compared to the n-charged case and simultaneously increased Q_r by 10 to fix the absolute values of q_k to those of the electron case. High energy spectral weight is transferred to lower frequencies in p-charged QDs by two effects that both decrease spin fluctuation of the central spin on short time scales: (i) the increase of λ and (ii) the introduced energy splitting to the nuclei due to QC. The linewidth of the added Lorentzian (dot-dashed line) for fitting the Q_r spectra corresponds to a lifetime $T_H = 497$ ns.

Figure 2 also provides a direct comparison between electron and hole spin noise. Since the Overhauser peak, which is present in the electron and absent in the hole spin

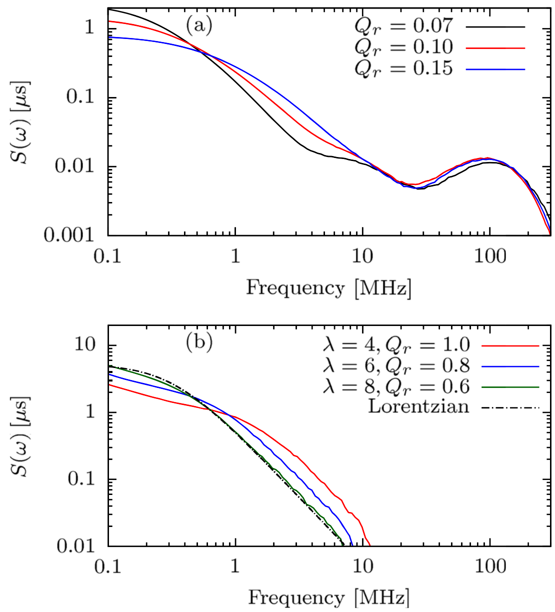

FIG. 2 (color online). Spin noise spectra of an electron spin (a) and a hole spin (b) for various combinations of Q_r and the hole anisotropy parameter λ. For the $Q_r = 0.6$ hole spectrum we supplemented a Lorentzian (dot-dashed line) corresponding to a lifetime $T_H \approx 500$ ns.

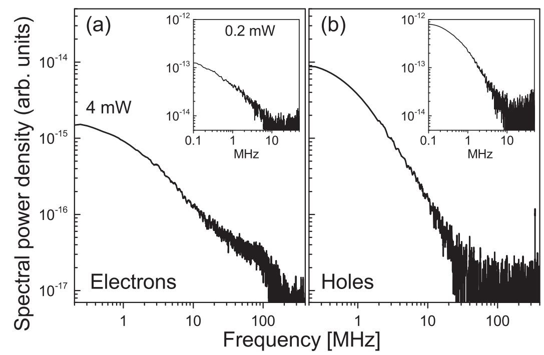

FIG. 3. Measured spin noise spectra at zero external magnetic field for electron (a) and hole spins (b) in ensembles of single charged QDs, measured around 890 nm laser excitation wavelength at 4 mW power level. The insets show measurements at 0.2 mW laser power.

noise spectrum, contains approximately 2/3 of the total spectral weight of $S(\omega)$ and the sum rule (4) must always be obeyed, the low frequency signal for electrons must be a factor of 3 smaller than for holes.

Lorentzian fits to the hole spin spectra for $Q_r = 0.8, \lambda = 6$ and $Q_r = 1.0$, $\lambda = 4$ yield the spin lifetimes $T_H = 265$ ns and $T_H = 144$ ns, which matches the finding $T_H = 188$ ns for electron spins at $Q_r = 0.1$ extremely well. Although the hole noise spectra lack the peak at large frequencies and their shapes are slightly different, the decrease of the low frequency spectrum occurs at the same order of magnitude for electron and hole spins provided by the same absolute QC strength demonstrating that the electron and hole lifetime are of the same order of magnitude. We stress that the details of the obtained spectra vary significantly for other semiconductor QDs than $In_xGa_{1-x}As$, $0.3 < x < 0.7$, but the qualitative agreement between the similar lifetime of electron and hole spins when doping the same material remains.

For further comparison with our calculation, Fig. 3 shows experimentally measured spin noise spectra at a temperature of 5 K. The experiments were performed on (In,Ga)As quantum dot ensembles of similar dot density, in one case on average doped by a single electron per dot, in the other case by a single hole [11,32]. The samples were studied using identical excitation conditions. The linearly polarized light beam of a single frequency laser was tuned to the ground state transition energy maximum [11].

The comparison of the electron and hole spin noise spectra in Figs. 3(a) and 3(b) with the calculations reveals that the theory qualitatively correctly predicts the shape and widths of the spin-noise spectra. In particular, the following features are worth noting. (i) The electron spin noise shows an additional peak around 100 MHz unveiling the electron's precession in the frozen Overhauser field [7], as also present in Fig. 1(b). Its reduction compared to the theory is related to a mixture of 80% n-charged and 20% p-charged QD in the sample. This ratio was determined by spin noise studies in a magnetic field transverse to the optical axis. Because of their different g factors, resulting in different Larmor precession frequencies, the corresponding noise peaks appear at very different frequencies in the noise spectrum. From the ratio of these noise peak areas the fraction of n- and p-doped dots can be assessed. (ii) Since $S(\omega)$ must obey the sum rule (4), the low-frequency spectral weight of $S(\omega)$ for n-charged QD is only about 1/3 of those for holes. A Lorentzian fit to the low frequency components ($f < 35$ MHz) of the experimental data confirms this difference in the amplitudes. (iii) A spin correlation time of the same order of magnitude in the long-time range for electrons and hole spins, as predicted by the theory. In the experiment this time is on the order of 400 ns, as estimated from the peak width at low frequencies.

Summary.—We have compared the impact of the hyperfine interaction on the spin coherence in n- and p-charged QDs, including the nuclear quadrupolar electric interaction generated by the strain fields, which provides an additional decoherence mechanism acting equally for n- and p-charged QDs. This mechanism is sufficient to explain the very similar long-time decay time T_H of n- and p-charged QDs. On the other hand, the different coupling of electron and hole spins in the central spin part of the Hamiltonian leads to significant deviations in the short term dynamics, most prominently evidenced by the electron spin precession about the nuclear magnetic field.

The samples have been provided by D. Reuter and A. D. Wieck, Ruhr-University Bochum, Germany. This work has been supported by the DFG and the RFBR through the transregio TRR 160. We acknowledge support by the BMBF through Q.com-HL.

[1] A. Khaetskii, D. Loss, and L. Glazman, Phys. Rev. B **67**, 195329 (2003).
[2] A. Greilich, D. R. Yakovlev, A. Shabaev, A. L. Efros, I. A. Yugova, R. Oulton, V. Stavarache, D. Reuter, A. Wieck, and M. Bayer, Science **313**, 341 (2006).
[3] R. Hanson, L. P. Kouwenhoven, J. R. Petta, S. Tarucha, and L. M. K. Vandersypen, Rev. Mod. Phys. **79**, 1217 (2007).
[4] J. Fischer, W. A. Coish, D. V. Bulaev, and D. Loss, Phys. Rev. B **78**, 155329 (2008).
[5] F. Jelezko, T. Gaebel, I. Popa, A. Gruber, and J. Wrachtrup, Phys. Rev. Lett. **92**, 076401 (2004).
[6] F. Jelezko and J. Wrachtrup, Phys. Status Solidi (a) **203**, 3207 (2006).
[7] I. A. Merkulov, A. L. Efros, and M. Rosen, Phys. Rev. B **65**, 205309 (2002).
[8] W. A. Coish and D. Loss, Phys. Rev. B **70**, 195340 (2004).
[9] M. Gaudin, J. Phys. (Paris) **37**, 1087 (1976).
[10] C. Testelin, F. Bernardot, B. Eble, and M. Chamarro, Phys. Rev. B **79**, 195440 (2009).
[11] S. A. Crooker, J. Brandt, C. Sandfort, A. Greilich, D. R. Yakovlev, D. Reuter, A. D. Wieck, and M. Bayer, Phys. Rev. Lett. **104**, 036601 (2010).
[12] D. Press, K. D. Greve, P. McMahon, T. Ladd, B. Friess, C. Schneider, M. Kamp, S. Hoefling, A. Forchel, and Y.Yamamoto, Nat. Photonics **4**, 367 (2010).
[13] K. D. Greve, P. L. McMahon, D. Press, T. D. Ladd, D. Bisping, C. Schneider, M. Kamp, L.Worschech, S. Höfling, A. Forchel, and Y. Yamamoto, Nat. Phys. **7**, 872 (2011).
[14] S. Varwig, A. Schwan, D. Barmscheid, C. Müller, A. Greilich, I. A. Yugova, D. R. Yakovlev, D. Reuter, A. D. Wieck, and M. Bayer, Phys. Rev. B **86**, 075321 (2012).
[15] A. Bechtold, A. Rauch, T. Simmet, P.-L. Ardelt, A. Regler, K. Müller, N. A. Sinitsyn, and J. J. Finley, Nat. Phys. (in press).
[16] R. V. Pound, Phys. Rev. **79**, 685 (1950); A. Abragam, *The Principles of Nuclear Magnetism* (Clarendon Press, Oxford, 1961); C. P. Slichter, *Principles of Magnetic Resonance* (Springer Science & Business Media, Berlin, 1996).
[17] E. A. Chekhovich, K. V. Kavokin, J. Puebla, A. B. Krysa, M. Hopkinson, A. D. Andreev, A. M. Sanchez, R. Beanland, M. S. Skolnick, and A. I. Tartakovskii, Nat. Nanotechnol. **7**, 646 (2012).
[18] K. Flisinski, I. Y. Gerlovin, I. V. Ignatiev, M. Y. Petrov, S. Y. Verbin, D. R. Yakovlev, D. Reuter, A. D. Wieck, and M. Bayer, Phys. Rev. B **82**, 081308 (2010); M. S. Kuznetsova, K. Flisinski, I. Y. Gerlovin, M. Y. Petrov, I. V. Ignatiev, S. Y. Verbin, D. R. Yakovlev, D. Reuter, A. D. Wieck, and M. Bayer, *ibid.* **89**, 125304 (2014).
[19] E. Welander, E. Chekhovich, A. Tartakovskii, and G. Burkard, arXiv:1405.1329.
[20] E. A. Chekhovich, M. Hopkinson, M. S. Skolnick, and A. I. Tartakovskii, Nat. Commun. **6**, 1 (2015).
[21] N. A. Sinitsyn, Y. Li, S. A. Crooker, A. Saxena, and D. L. Smith, Phys. Rev. Lett. **109**, 166605 (2012).
[22] C. Bulutay, Phys. Rev. B **85**, 115313 (2012); C. Bulutay, E. A. Chekhovich, and A. I. Tartakovskii, *ibid.* **90**, 205425 (2014).
[23] J. Hackmann and F. B. Anders, Phys. Rev. B **89**, 045317 (2014).
[24] K. A. Al-Hassanieh, V. V. Dobrovitski, E. Dagotto, and B. N. Harmon, Phys. Rev. Lett. **97**, 037204 (2006).
[25] G. Chen, D. L. Bergman, and L. Balents, Phys. Rev. B **76**, 045312 (2007).
[26] D. Smirnov, M. Glazov, and E. Ivchenko, Phys. Solid State **56**, 254 (2014).
[27] G. S. Uhrig, J. Hackmann, D. Stanek, J. Stolze, and F. B. Anders, Phys. Rev. B **90**, 060301 (2014).
[28] M. M. Glazov and E. L. Ivchenko, Phys. Rev. B **86**, 115308 (2012).
[29] A. Faribault and D. Schuricht, Phys. Rev. Lett. **110**, 040405 (2013).
[30] R. Dahbashi, J. Hübner, F. Berski, J. Wiegand, X. Marie, K. Pierz, H. W. Schumacher, and M. Oestreich, Appl. Phys. Lett. **100**, 031906 (2012).
[31] Y. Li, N. Sinitsyn, D. L. Smith, D. Reuter, A. D. Wieck, D. R. Yakovlev, M. Bayer, and S. A. Crooker, Phys. Rev. Lett. **108**, 186603 (2012).
[32] V. S. Zapasskii, A. Greilich, S. A. Crooker, Y. Li, G. G. Kozlov, D. R. Yakovlev, D. Reuter, A. D. Wieck, and M. Bayer, Phys. Rev. Lett. **110**, 176601 (2013).
[33] H. Tal-Ezer and R. Kosloff, J. Chem. Phys. **81**, 3967 (1984).
[34] V. V. Dobrovitski and H. A. De Raedt, Phys. Rev. E **67**, 056702 (2003).
[35] A. Weiße, G. Wellein, A. Alvermann, and H. Fehske, Rev. Mod. Phys. **78**, 275 (2006).
[36] See Supplemental Material at http://link.aps.org/supplemental/10.1103/PhysRevLett.115.207401, which includes Refs. [37–51], for a brief summary of the derivation of the anisotropic central spin model and known properties of the nuclear electric quadrupolar interaction.
[37] M. Bortz and J. Stolze, Phys. Rev. B **76**, 014304 (2007).
[38] M. Bortz, S. Eggert, and J. Stolze, Phys. Rev. B **81**, 035315 (2010).
[39] A. Faribault and D. Schuricht, Phys. Rev. B **88**, 085323 (2013).
[40] D. Stanek, C. Raas, and G. S. Uhrig, Phys. Rev. B **88**, 155305 (2013).
[41] U. Schollwöck, Ann. Phys. (Amsterdam) **326**, 96 (2011).
[42] E. Fermi, Z. Phys. **60**, 320 (1930).
[43] S. Lee, P. von Allmen, F. Oyafuso, G. Klimeck, and K. B. Whaley, J. Appl. Phys. **97**, 043706 (2005).
[44] S. Schulz, D. Mourad, and G. Czycholl, Phys. Rev. B **80**, 165405 (2009).
[45] D. Mourad, S. Barthel, and G. Czycholl, Phys. Rev. B **81**, 165316 (2010).
[46] P. Mazur, Physica (Utrecht) **43**, 533 (1969).
[47] P. Reimann, Phys. Rev. Lett. **101**, 190403 (2008).
[48] M. Rigol and M. Srednicki, Phys. Rev. Lett. **108**, 110601 (2012).
[49] M. Römer, J. Hübner, and M. Oestreich, Rev. Sci. Instrum. **78**, 103903 (2007).
[50] G. M. Müller, M. Römer, D. Schuh, W. Wegscheider, J. Hübner, and M. Oestreich, Phys. Rev. Lett. **101**, 206601 (2008).
[51] S. A. Crooker, L. Cheng, and D. L. Smith, Phys. Rev. B **79**, 035208 (2009).
[52] R. I. Dzhioev and V. L. Korenev, Phys. Rev. Lett. **99**, 037401 (2007).
[53] P. S. Sokolov, M. Y. Petrov, T. Mehrtens, K. Müller-Caspary, A. Rosenauer, D. Reuter, and A. D. Wieck, arXiv:1508.07957.